IEEE Photonics Journal
An IEEE Photonics Society Publication

Open Access

Source Location and Suppression of Phase Induced Intensity Noise in Fiber-Based Continuous-Wave Coherent Doppler Lidar

Volume 13, Number 3, June 2021

Zheng Tang
Mengfan Wang
Wei Feng
Xiaoyuan Sun
Benli Yu
Kai Qian
Ping Chen
Guojie Tu

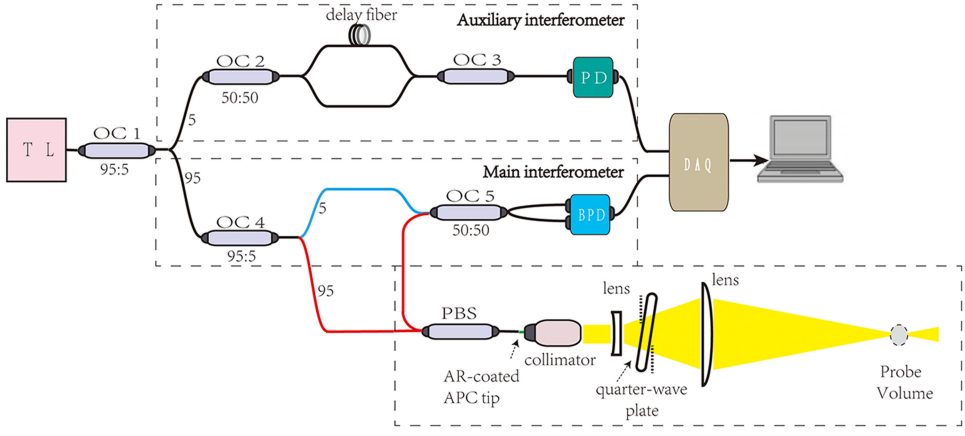

DOI: 10.1109/JPHOT.2021.3078769

Source Location and Suppression of Phase Induced Intensity Noise in Fiber-Based Continuous-Wave Coherent Doppler Lidar

Zheng Tang,[1,2] Mengfan Wang,[1,2] Wei Feng,[1,2] Xiaoyuan Sun,[1,2] Benli Yu,[1,2] Kai Qian,[3] Ping Chen,[4] and Guojie Tu[1,2]

[1]Information Materials and Intelligent Sensing Laboratory of Anhui Province, Anhui University, Hefei 230601, China
[2]Key Laboratory of Opto-Electronic Information Acquisition and Manipulation of Ministry of Education, Anhui University, Hefei 230601, China
[3]School of Advanced Materials and Mechatronic Engineering, Hubei Minzu University, Enshi 445000, China
[4]Energy Group Qiyueshan Wind Power Company, Ltd., Lichuan 445400, China

DOI:10.1109/JPHOT.2021.3078769

Manuscript received January 29, 2021; revised April 28, 2021; accepted May 5, 2021. Date of publication May 11, 2021; date of current version May 28, 2021. This work was supported in part by the National Key Research and Development Program 2016YFC0301900, in part by the University Synergy Innovation Program of Anhui Province (GXXT-2020-052), and in part by the National Natural Science Foundation of China under Grants 61705001, 61905001, and 61665002. Corresponding author: Guojie Tu (e-mail: 15041@ahu.edu.cn).

Abstract: The phase induced intensity noise (PIIN) may seriously reduce the signal-to-noise ratio (SNR) of continuous-wave coherent Doppler lidar (CW-CDL), thereby limiting its performance in practical applications. In this paper, we propose to use optical frequency domain reflectometry (OFDR) technique to locate the PIIN sources and evaluate their intensities. According to the OFDR information, we demonstrate that the PIIN in our CW-CDL system is mainly induced by the crosstalk of polarization beam splitter. Then, the PIIN is reduced by setting fiber delay line, polarization control, and AR-coating. Finally, a wind Doppler signal at a distance of 80 meters is obtained on a clear day, and a typical SNR of 19.4 dB is achieved.

Index Terms: Continuous-wave coherent Doppler lidar, phase induced intensity noise, optical frequency domain reflectometry.

1. Introduction

Coherent Doppler lidar (CDL) has been applied in many fields, such as wind measurement and vibration measurement [1]–[3]. With respect to wind measurement, due to its shorter wavelength, CDL is easier to obtain effective echo in clear sky than microwave wind radar [4], thus is has attracted more and more attention. In this technology, the weak Mie backscattering from the aerosol particle is mixed with the reference light on the photon detector, and then the wind velocity can be obtained according to the frequency of the beat signal output by the detector.

Since the early use of CO_2 laser source for wind measurement [5], CDL has experienced decades of development and made significant progress. The efforts of the researchers include the application of new light sources such as fiber laser with Erbium doped fiber amplifier (EDFA)

and all-semiconductor master-oscillator-power-amplifier (MOPA) [6], [7], different optical structures such as free-space [8] and all-fiber optics [9], and different data analysis methods [10]. It is worth noting that with the development of optical fiber communication industry, continuous-wave (CW) CDL with 1550 nm laser source and fiber-based optical path has many various advantages in typical applications such as wind field test, generator power curve test [11], [12]. First, 1550 nm has the characteristics of human eye safety, high maturity and low cost. Second, it is easier to achieve high stability in fiber-based optical path than in free-space optical path. Finally, pulse modulator is not needed in CW-CDL, which greatly reduces the cost. However, the CW-CDL system mentioned above also has some problems. For instance, in contrast to pulse-CDL, CW-CDL is not only affected by laser relative intensity noise (RIN), shot noise (SN) and detector noises [13], [14], but also by phase induced intensity noise (PIIN) caused by stray light such as device crosstalk light, reflected or scattered light from the optical path [15], [16]. More seriously, PIIN usually exceeds other noises and becomes the main limitation of system performance.

In CW-CDL system, the PIIN noise refers to the fluctuation of the output of photon detector induced by the random phase noise of the laser source. Generally, when the optical path difference (OPD) between stray light and reference light is significantly shorter than the coherence length of the laser, the PIIN will appear as white noise floating in the signal spectrum, thus reducing the signal-to-noise ratio (SNR) of the system. To solve the PIIN problem, P. Rodrigo *et al.* reported a polarization control method based on single-mode fiber-based optical path in 2010 [17]. After 90-degree rotation of the polarization state of backscattered light and reference light, the PIIN noise caused by the leakage of 1-3 ports of the optical circulator was reduced by about 20 dB, which makes the wind velocity measurement more reliable. It should be noted that similar polarization control method has also been used to suppress the PIIN in the free-space based CW-CDL [18]. In addition, methods such as anti-reflection (AR) coating on the surface of optical devices, tilt mounting of lenses, and shortening the OPD between stray light and reference light have also been widely used to suppress PIIN in CW-CDL [17], [18]. However, as far as we know, in previous reports, PIIN was evaluated by measuring the noise spectrum background, rather than by directly measuring the stray light. In other words, for a CW-CDL system with multiple PIIN sources, it is difficult to evaluate the impact of each PIIN source on the system, which makes it difficult to fully optimize the system.

Recently, we have focused on reducing the noise in CW-CDL, and developed a method to evaluate the PIIN source based on optical frequency domain reflectometry (OFDR). By using OFDR to accurately locate the stray light and measure its intensity, we have realized the direct measurement of PIIN source in CW-CDL, which provides an accurate basis for the noise suppression of the system. In this paper, we first introduce the noises in CW-CDL and some suppression methods. Next, the OFDR system and how to use the system to obtain the position and intensity of the stray light are introduced. Then, according to the information provided by OFDR, the SNR of our CW-CDL system is confirmed to be mainly affected by the crosstalk of polarization beam splitter (PBS). Finally, using the optimized CW-CDL system, the wind Doppler signal with a SNR of 19.4 dB is obtained.

2. Principle

2.1 Noises in CW-CDL

Several noise sources have to be considered in a CW-CDL system. Some of the noises are related to photon detector, including thermal noise (TN) and dark current noise (DCN). On the other hand, other noises are related to light source, including SN, RIN and PIIN. Among them, the mean square value of the photon current induced by PIIN can be described as [19]:

$$\left\langle {i_p}^2 \right\rangle = \Re^2 \frac{2P_r P_{st} l_c}{\pi c} \left[1 - \exp\left(-\frac{l_d}{l_c} \right) \left(1 + \frac{l_d}{l_c} \right) \right] B \tag{1}$$

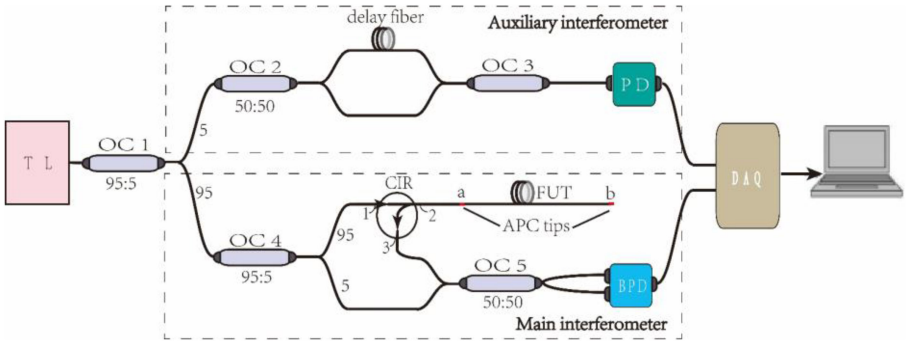

Fig. 1. The typical setup of optical frequency domain reflectometry (OFDR). TL: tunable laser; OC: optical coupler; CIR: circular; FUT: fiber under test; PD: photon detector; BPD: balanced photon detector; DAQ: data acquisition card, the sampling length is 5×10^4.

Where $\Re$ is the responsivity of the photon detector, P_r and P_{st} are the intensities of the reference light and stray light respectively, l_d denotes the OPD between stray light and reference light, l_c represents the coherence length of the laser source, and B is the resolution bandwidth of the system.

For CW-CDL system, l_d is usually much shorter than l_c, which indicates that the PIIN will behave as white noise and Eq. (1) can be simplified as follows:

$$\left\langle i_p^2 \right\rangle = \Re^2 \frac{2P_r P_{st}}{\pi c} \frac{{l_d}^2}{l_c} B \tag{2}$$

Therefore, when all the above noises are taken into account and the balanced photon detector (BPD) is used, the SNR of the system satisfies the following relationship:

$$SNR = \frac{\Re^2 P_{ms} P_r}{\frac{2kTB}{R} + 2e(P_r\Re + i_d)B + \frac{\alpha {P_r}^2 \Re^2 B}{\beta} + \frac{\Re^2 P_r P_{st} {l_d}^2 B}{\pi c l_c}} \tag{3}$$

Here P_{ms} is the intensity of the signal light (Mie scattering light for a wind measurement system), k and T denote the Boltzmann constant and the temperature respectively, R is the equivalent internal resistance of the detector, e and i_d represent the electron quantity and the dark current of the detector, α is the RIN factor, and β is the common mode rejection ratio of the balanced detection. It can be seen that, when PIIN is much stronger than other noises, the SNR can be rewritten as:

$$SNR = \frac{\pi c l_c P_{ms}}{P_{st} {l_d}^2 B} \tag{4}$$

It can be seen from Eq. (4) that some methods can be used to improve the SNR. First, the power of signal light P_{ms} can be improved by increasing the telescope aperture or the power of probe light. Second, resolution bandwidth B can be reduced by average calculation. At last, reducing the stray light intensity P_{st} or shortening l_d [20] can also reduce the PIIN and improve the SNR. In a practical CW-CDL system, it is necessary to combine the above methods to achieve the best SNR, and we will focus on reducing P_{st} and l_d in this paper.

2.2 OFDR

We propose the OFDR technique to accurately evaluate P_{st} and l_d. OFDR can be understood as frequency modulated continuous wave (FMCW) system operating in optical fiber [21]–[23]. The typical structure is shown in Fig. 1. The CW laser emitted by the tunable laser (TL) is divided into two beams by the coupler and injected into the main interferometer and the auxiliary interferometer, respectively. The output of the detector in the auxiliary interferometer is used as the external clock

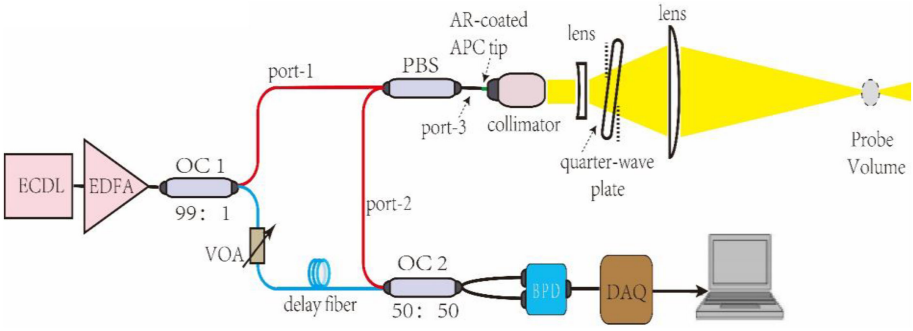

Fig. 2. The experimental setup of fiber-based CW-CDL for wind measurement. ECDL: external cavity diode laser; EDFA: Erbium doped fiber amplifier; PBS: polarization beam splitter.

of the data acquisition card (DAQ) to realize the correction of nonlinear laser tuning. The beam in the main interferometer is also divided into two parts, one is used as the reference light, and the other is used as the probe light. The back propagated light from distance x will pass through the optical circulator again and arrive at the BPD together with the reference light to generate beat signal [22]:

$$I(t) = 2\Re\sqrt{P_r P_{os}}\cos\left(\frac{4\pi n\gamma xt}{c} + \phi\right) \tag{5}$$

Where P_{os} denotes the intensity of the signal light of OFDR system. Note that when using OFDR to monitor the PIIN source in CW-CDL, the signal light includes stray light such as crosstalk or reflection of optical devices. In addition, n represents the refractive index of sensing medium, γ and c denote the laser frequency scanning speed and the light speed in vacuum respectively, and φ is a random phase.

It can be seen that the frequency of $I(t)$ depends on x, thus it can be used to locate the stray light. Moreover, P_{os} can be obtained by calculating the power of the signal with a frequency of $2n\gamma x/c$, which means that the intensity of stray light (P_{st}) in Eq. (4) can also be evaluated by OFDR.

3. Experimental Setup of CW-CDL

The optimized setup of fiber-based CW-CDL is shown in Fig. 2. An external cavity diode laser (ECDL) provides a CW seed light of 6 mW at 1550 nm, the wavelength stability is $\pm$0.05 nm, and the bandwidth is less than 20 kHz, indicating a coherent length of about 15 km. The output of EDFA is divided into two parts by a 99:1 optical coupler (OC1). The 1% part is first reduced to about 400 μW by a variable optical attenuator (VOA). Then it passes through a delay fiber and acts as the reference light in the coherent system. The 99% part with a power of about 385 mW is used as the probe light. The probe light first enters the port-1 of a polarization beam splitter (PBS), and then enters a collimator through port-3 and an AR coated APC tip. The collimator outputs a beam with a diameter of 3 mm, which then reaches a telescope composed of a plano-concave lens and a plano-convex lens. The aperture of the telescope is 50 mm. The probe beam is focused 80 m ahead. A quarter-wave plate with a fast axis of 45 degree to the polarization direction is installed between the plano-concave lens and plano-convex lens to adjust the polarization state of the probe light. The qurter-wave plate is slightly tilted to avoid any reflected light. The Mie scattering light caused by aerosol particles passes through telescope, quarter-wave plate and collimator, and finally returns to port-3 of PBS, with a polarization state rotating 90 degrees. Then it passes through port-2 of PBS, enters into a 3 dB optical coupler (OC2) and mixes with the reference light at a BPD with a bandwidth of 50 MHz. The output of BPD is sampled by DAQ card with a sampling rate

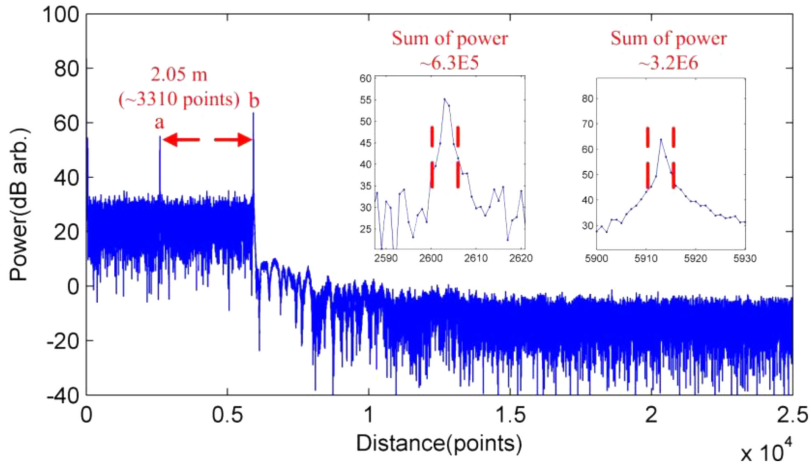

Fig. 3. The OFDR spectrum of 2.05 m polarization maintaining fiber (PMF). A spatial resolution (SR) of 0.62 mm can be observed, and the light intensities of APC reflections are shown in the insets.

of 80 MS/s. The fast Fourier transform (FFT) and average calculation are implemented by a field programmable gate array (FPGA) in DAQ card to obtain the signal spectrum.

The above system has made some optimizations to the reported CW-CDL. First, the optical circulator is replaced by PBS [3], [16], thus most of reflected light from the collimator and telescope can be eliminated by polarization selection, which can reduce P_{st}. Second, in our system, the reference light and the probe light are separated after the EDFA, rather than after the seed light as usual [23], therefore accurate measurement of I_d can be achieved. Finally, the quarter-wave plate is placed between the plano-concave lens and plano-convex lens, which can further reduce P_{st} from the plano-concave lens without increasing the cost.

4. Experiment and Results

4.1 Calibration of OFDR

A 2.05 m polarization maintaining fiber (PMF, FUT a-b in Fig. 1) is firstly used to calibrate the OFDR system. In our OFDR system, a tunable laser (New focus, TLB 6728) provides 10 mW output with a linewidth of 200 kHz, and the tuning rate is 10 nm/s. The delay fiber of the auxiliary interferometer is 31 meters, and the bandwidth of the BPD (Thorlabs, PDB 450C) is 4 MHz. In order to calculate the spatial resolution (SR), a sawtooth signal with a peak to peak value of 4 V and a frequency of 1 Hz is collected. The collected signal presents a monotonic curve with the maximum voltage difference of 1.024 V, thus we infer that it takes about 0.128 s to sample 5×10^4 points with the external clock. Therefore, the effective tuning range is 1520-1521.28 nm owing to the tuning rate of 10 nm/s, and the theoretical spatial resolution (SR) of about 0.6 mm (in fiber) and 0.9 mm (in air) can be predicted [24] by the following formula:

$$\Delta z = \frac{\lambda^2}{2n\Delta\lambda} \tag{6}$$

where λ and $\Delta\lambda$ denote the wavelength and tuning range of the TL, respectively.

The result of calibration experiment is shown in Fig. 3. The marked points *a* and *b* with a horizontal axis spacing of 3310 points are derived from the reflections of APC tips of FUT. Therefore, the measured SR of OFDR is 0.62 mm, which is well consistent with the theoretical value calculated by Eq. (6). Besides, by calculating the power of the two peaks, the APC reflection intensities are also shown in the insets, which are 6.3×10^5 and 3.2×10^6 , respectively. In the following sections, the actual distance of any optical devices can be obtained by calculating the

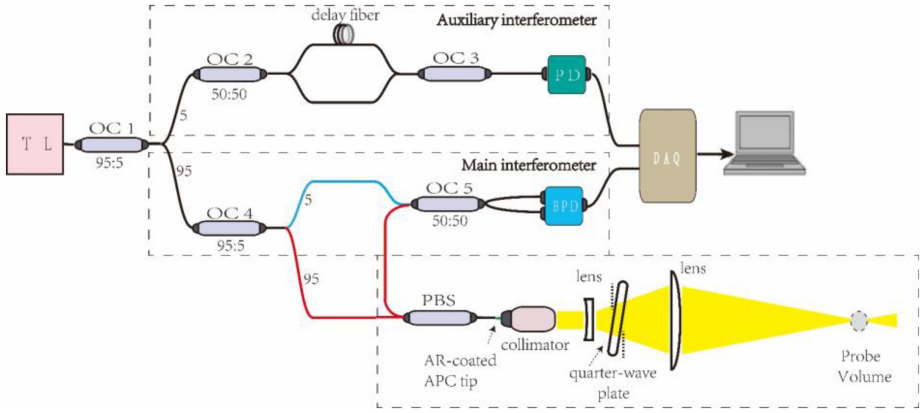

Fig. 4. The measurement of PIIN sources of fiber-based CW-CDL using OFDR.

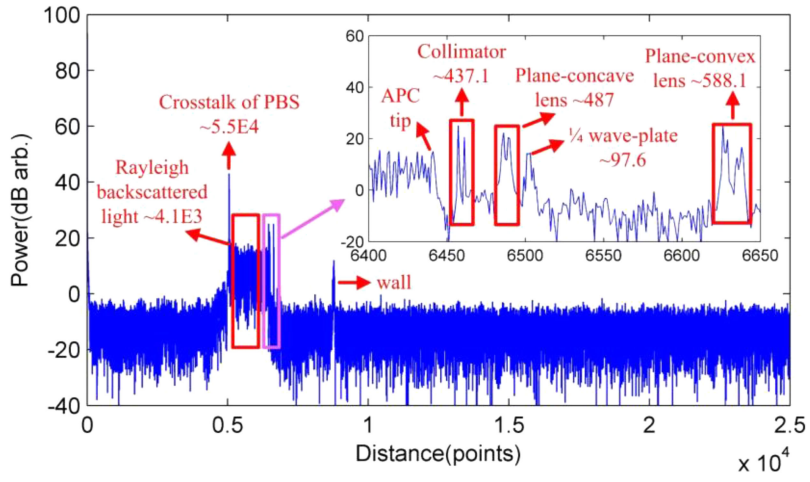

Fig. 5. The measurement result of PIIN sources, which indicates that the crosstalk of PBS is the main PIIN source.

product of SR and the horizontal axis interval of devices, and the intensity of crosstalk, reflected or scattered light can be accurately calculated according to the above method.

4.2 Analysis of PIIN Sources Using OFDR

The experimental setup shown in Fig. 4 is used to locate the PIIN sources and evaluate their intensities. The optical transmitting/receiving part of CW-CDL is transplanted to the corresponding position of OFDR system. Then, the crosstalk from port-1 to port-2 of PBS, the reflected and scattered light of optical devices can be directly observed by OFDR. The results are shown in Fig. 5. It can be seen that there are about 5000 points gaps before the PBS, indicating that the optical path of reference light (blue line) is about 6.2 m shorter than that of crosstalk of PBS (red line). It should be noted that the crosstalk light propagates forward, thus the SR in front of PBS is twice the value obtained by Eq. (6), which is about 1.2 mm. In addition, as we expected, other devices in the optical path are clearly shown in the figure, such as the reflections of collimator and the surfaces in the telescope. The OFDR spectrum behind the APC tip is pointed out by a pink window and enlarged in the inset. With the help of the high SR, the front and rear surfaces of collimator, plano-concave lens and plano-convex lens are all visible. For instance, the distance between the front and rear surfaces of the plano-concave lens is 3∼4 points, and the corresponding thickness

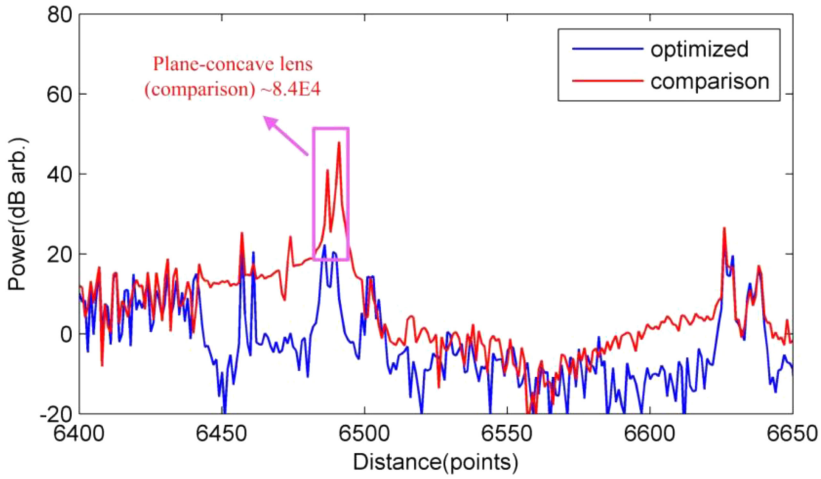

Fig. 6. The OFDR results of different optical paths. The quarter-wave plates are placed between the collimator and plano-concave lens in comparison system (red line) and between plano-concave and plano-convex lens in optimized system (blue line). It is observed that the PIIN is hard to suppress in comparison system, since the crosstalk of PBS and reflection of plano-concave lens are both strong.

is about 2 mm, which is consistent with the actual value. It is also observed that the front and rear surfaces of the quarter-wave plate cannot be distinguished, due to its slight tilt. Furthermore, referring to the calculation method of P_{st} in Fig. 3, the intensity of each PIIN source is accurately marked. Comparing the reflection intensities of two APC tips in Fig. 3, it can be seen that the APC reflection has been reduced to about Rayleigh scattering level by AR coating, which indicates that a strong PIIN source has been eliminated. The data also clearly show that the intensity of PIIN induced by crosstalk of PBS is 5.5×10^4, which is much higher than that caused by the reflection of other devices. Therefore, the crosstalk can be identified as the main source of PIIN noise in our CW-CDL. As a result, only the crosstalk of PBS should be considered to suppress PIIN, i.e., the delay fiber should be set according to the position of PBS, so as to effectively reduce l_d and PIIN.

OFDR can also provide real-time monitoring for the adjustment of optical transmitting/receiving part of CW-CDL system. It is found that the position of quarter-wave plate will affect the PIIN optimization of the system. Fig. 6 shows OFDR data when the quarter-wave plate is placed between the collimator and plano-concave lens (comparison, red line) and between plano-concave lens and plano-convex lens (optimized, blue line). Obviously, it is hard to eliminate the reflected light of plano-concave lens in the comparison system. As a result, the intensity of PIIN caused by the plano-concave lens in the comparison system (8.4×10^4) is much higher than that in the optimized system (487). Moreover, due to the spectrum leakage of OFDR system, the strong plano-concave lens induced PIIN leads to a large increase of OFDR spectrum in front of plano-concave lens. In other words, there are two strong PIIN sources in the comparison system, which are crosstalk of PBS and reflected light of plano-concave lens, respectively. Therefore, it is difficult to reduce the PIIN in comparison system, since the delay fiber cannot be set according to the positions of PBS and plano-concave lens at same time. It should be noted that, if the quarter-wave plate is placed behind the plano-convex lens, the reflection of the plano-convex lens can also be eliminated, but the reflection is much lower than that of the plano-concave lens, and the aperture of the quarter-wave plate needs to be increased, thus increasing the system cost.

4.3 Shortening the OPD Between Stray Light and Reference Light

Once it is confirmed that the main PIIN source is the crosstalk of PBS, it can be further suppressed by reducing the OPD between stray light and reference light (l_d in Eq. (4) or the difference of red

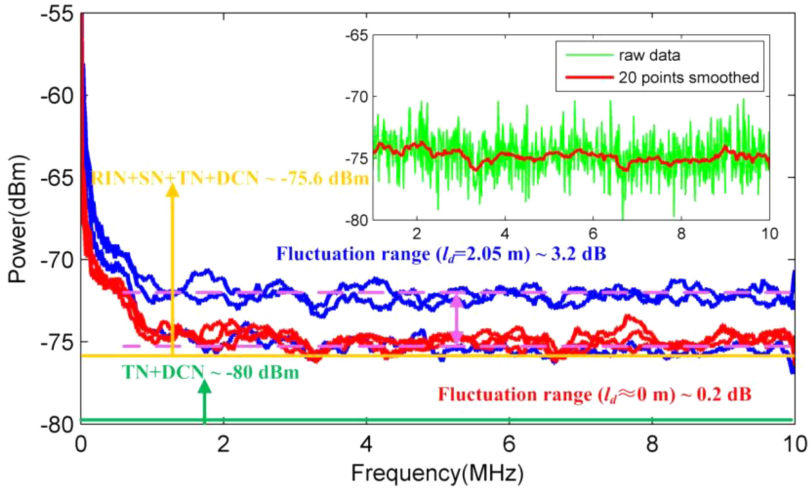

Fig. 7. The comparison of CW-CDL noises with different OPDs between stray light and reference light. The results show that the PIIN is effectively suppressed in the optimized system.

and blue lines in Fig. 2). Fig. 7 shows the floating noises floor at $l_d = 2.05$ m (comparison, blue line) and $l_d \approx 0$ m (optimized, red line) conditions, respectively. Note that both values of l_d are much smaller than the coherence length of the laser l_c, which means that the PIINs will behave as white noises. In the experiment, the output window of the telescope is covered by a black light absorbing plate to prevent additional strong PIIN source. The data is provided by a spectrum analyzer with a RBW of 1 kHz. The span is set to 10 MHz to shorten the sweep time. In addition, the data has been smoothed by 20 points for clarity, and the typical raw data is shown in the inset (only shows the frequency above 1 MHz, corresponding to the line-of-sight wind velocity $>$0.7 m/s). Some typical noise floors are also shown in the figure. The floor of -80 dBm is obtained when all the input light of the detector is blocked, thus it is composed of TN and DCN of the detector. The other floor at -75.6 dBm is obtained when the detector has only reference light input. Therefore, it is mainly caused by SN (with a theoretical value of -77 dBm) and residual RIN. It is observed that the PIIN fluctuates in the range of -75 to -72 dBm (the fluctuation range is about 3.2 dB) when $l_d = 2.05$ m, which can be explained by the instability of the phase difference between stray light and reference light [3]. In contrast, owing to the shorter balance state, the PIIN of the optimized CW-CDL system is stable at around -75 dBm (the fluctuation range is about 0.2 dB), which is very close to RIN and SN levels, thus proving the proposed method. It should be noted that the improved noise characteristics do not completely conform to Eq. (4), since the system has been operating close to the state without PIIN, *i.e.*, other noises such as residual RIN and SN have become obvious.

4.4 Evaluation of Polarization Control

The performance of polarization control method is also experimentally evaluated. The optimized CW-CDL system shown in Fig. 2 is compared with the CW-CDL system of traditional circulator scheme (the circulator replaces PBS and removes a quarter-wave plate). The delay fibers are set according to the positions of PBS and optical circulator, respectively. The output window of the telescope is also covered. The red and blue lines in Fig. 8 represent typical noise floor spectrums of optimized and traditional systems, which have also been smoothed by 20 points. The results show that, compared with the stable noise floor of around -75 dBm (the fluctuation range is about 0.2 dB) in the optimized CW-CDL system, the noise floor in the traditional CW-CDL system fluctuates irregularly in the range of -74.7 to -72.3 dBm (the fluctuation range is about 2.4 dB), which proves a great noise suppression by polarization control.

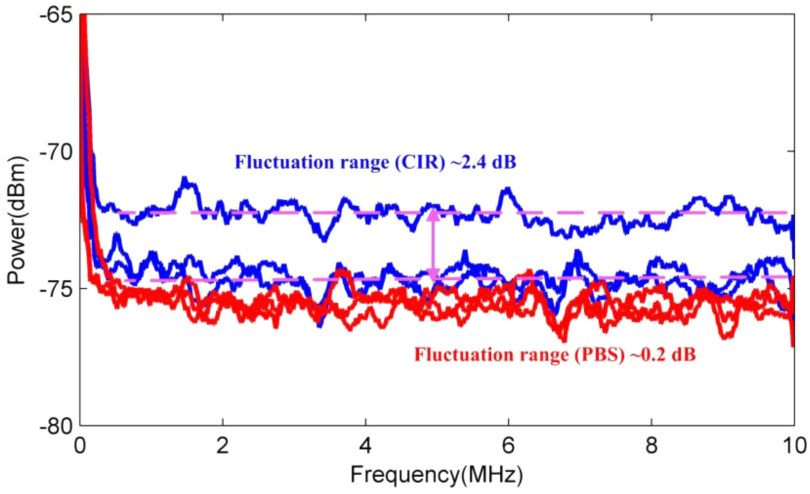

Fig. 8. The comparison of CW-CDL noises with and without polarization control.

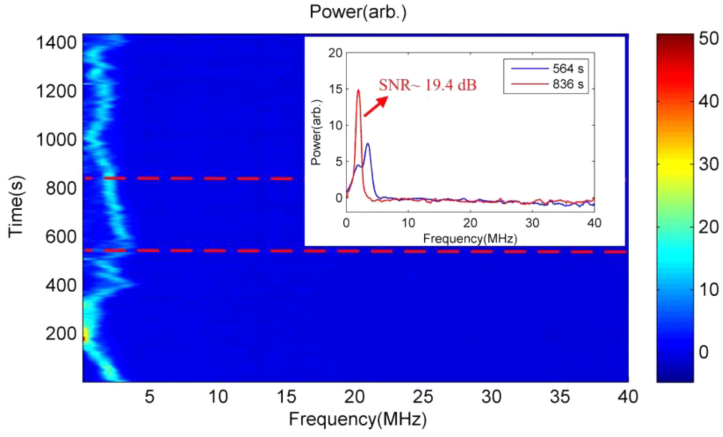

Fig. 9. Typical wind Doppler signal at 40 meters altitude on a clear day.

4.5 Measurement of Line-of-Sight Wind Velocity

Finally, using the optimized system, a typical wind Doppler signal at 40 meters altitude is obtained under clear sky condition. In the experiment, the focusing distance of the telescope is 80 m and diameter of the focal spot is about 0.8 cm. The DAQ card is AC coupling, the DAQ rate is 80 MS/s and the sample points is 1024, which indicates a RBW of 80 kHz. The maximum line-of-sight wind velocity is about 30 m/s, and the velocity resolution is around 0.12 m/s. Note that the accuracy of line-of-sight velocity measurement can be improved with the help of data fitting. The Doppler spectrum is averaged 10000 times, and the single measurement time is 125 ms. The signal is recorded for 1400 seconds, then the spectrum-time map is shown in Fig. 9. There are a lot of fluctuations and broadening of spectrum due to the instability of wind velocity. Two typical sets of Doppler spectrums marked by red lines are shown in the set. Among them, the wind velocity at 836 second is relatively stable, thus the spectrum is narrow. In this case, the SNR is 19.4 dB, which is obtained by calculating the ratio of the signal height to the standard deviation of noise floor [8]. As a comparison, due to the fluctuation of wind field during the measurement time, the wind spectrum broadened at 564 second. The superposition of two spectral peaks can be observed in the figure, resulting in the reduction of SNR.

5. Conclusion

The PIIN may seriously affect the SNR of a fiber-based CW-CDL system, and limits the practicability of this kind of lidar. In this paper, polarization control, AR-coating, and zero OPD between stray light and reference light design are used to reduce the PIIN. In order to locate the dominant PIIN source of the CW-CDL, OFDR system is introduced to measure the optical path. OFDR results show that the dominant PIIN source in the system is the crosstalk of PBS, which provides a direct basis for shortening the OPD between stray light and reference light. In addition, OFDR is also used to monitor the adjustment of the CW-CDL system, such as providing data support for the position selection of quarter-wave plate. It is experimentally demonstrated that the proposal can reduce the PIIN and improve the SNR in fiber-based CW-CDL, thus ensuring its ability to capture the wind Doppler signal in clear sky. Finally, due to the same basic principle, the proposal can also be simply extended to the development of CW-CDL systems operating in other applications, such as laser Doppler vibrometry.

References

[1] L. F. Du, G. T. Yang, J. H. Wang, C. Yue, and L. X. Chuan, "Implementing a wind measurement doppler lidar based on a molecular iodine filter to monitor the atmospheric wind field over Beijing," *J. Quant. Spectrosc. Radiative Transfer*, no. 188, pp. 3–11, 2017.

[2] D. P. Held and J. Mann, "Comparison of methods to derive radial wind speed from a continuous-wave coherent lidar doppler spectrum," *Atmospheric Meas. Tech.*, vol. 11, no. 11, pp. 6339–6350, 2018.

[3] C. J. Karlsson, F. A. Olsson, M. Harris, and D. Letalick, "All-fiber multifunction continuous-wave coherent laser radar at 1.55 μm for range, speed, vibration, and wind measurements," *Appl. Opt.*, vol. 39, no. 21, pp. 3716–3726, 2000.

[4] R. J. Barthelmie *et al.*, "Offshore wind turbine wakes measured by sodar," *J. Atmospheric Ocean. Technol.*, vol. 20, no. 4, pp. 466–477, 2003.

[5] R. M. Huffaker, "Laser doppler detection systems for gas velocity measurement," *Appl. Opt.*, vol. 9, no. 5, pp. 1026–1039, 1970.

[6] C. F. Abari, A. T. Pedersen, and J. Mann, "An all-fiber image-reject homodyne coherent doppler wind lidar," *Opt. Exp.*, vol. 22, no. 21, pp. 25880–25894, 2014.

[7] G. Arisholm, O. Nordseth, and G. Rustad, "Optical parametric master oscillator and power amplifier for efficient conversion of high-energy pulses with high beam quality," *Opt. Exp.*, vol. 12, no. 18, pp. 4189–4197, 2004.

[8] R. S. Hansen, and C. Pedersen, "All semiconductor laser doppler anemometer at 1.55 μm," *Opt. Exp.*, vol. 16, no. 22, pp. 18288–18295, 2008.

[9] C. Hill, "Coherent focused lidars for doppler sensing of aerosols and wind," *Remote Sens-basel*, vol. 10, no. 3, pp. 1–24, 2018.

[10] S. Jiang, D. S. Sun, Y. L. Han, F. Han, A. R. Zhou, and J. Zheng, "Performance of continuous-wave coherent doppler lidar for wind measurement," *Curr. Opt. Photon.*, vol. 3, no. 5, pp. 466–472, 2019.

[11] I. Antoniou, S. M. Pedersen, and P. B. Enevoldsen, "Wind shear and uncertainties in power curve measurement and wind resources," *Wind Eng.*, vol. 33, no. 5, pp. 449–468, 2010.

[12] R. Wagner, T. F. Pedersen, M. Courtney, I. Antoniou, S. Davoust, and R. L. Rivera, "Power curve measurement with a nacelle mounted lidar," *Wind Eng.*, vol. 17, no. 9, pp. 1441–1453, 2014.

[13] S. Kameyama, T. Ando, K. Asaka, Y. Hirano, and S. Wadaka, "Compact all-fiber pulsed coherent doppler lidar system for wind sensing," *Appl. Opt.*, vol. 46, no. 11, pp. 1953–1962, 2007.

[14] G. A. Cranch, M. A. Englund, and C. K. Kirkendall, "Intensity noise characteristics of erbium-doped distributed-feedback fiber lasers," *IEEE J. Quantum Electron.*, vol. 39, no. 12, pp. 1579–1587, Dec. 2003.

[15] M. Harris, G. N. Pearson, J. M. Vaughan, D. Letalick, and C. Karlsson, "The role of laser coherence length in continuous-wave coherent laser radar," *J. Mod. Opt.*, vol. 45, pp. 1567–1581, 1998.

[16] M. P. Van Exter, S. J. M. Kuppens, and J. P. Woerdman, "Excess phase noise in self-heterodyne detection," *IEEE J. Quantum Electron.*, vol. 28, no. 3, pp. 580–584, Mar. 1992.

[17] P. J. Rodrigo, and C. Pedersen, "Reduction of phase-induced intensity noise in a fiber-based coherent doppler lidar using polarization control," *Opt. Exp.*, vol. 18, no. 5, pp. 5320–5327, 2010.

[18] P. J. Rodrigo, and C. Pedersen, "Field performance of an all-semiconductor laser coherent doppler lidar," *Opt. Lett.*, vol. 37, no. 12, pp. 2277–2279, 2012.

[19] M. Harris, G. N. Pearson, J. M. Vaughan, D. Letalick, and C. Karlsson, "The role of laser coherence length in continuous-wave coherent laser radar," *J. Modern Opt.*, vol. 45, pp. 1567–1581, 1998.

[20] H. J. Zhou, W. Chen, Z. Meng, and C. F. Sun, "Phase noise characteristics of narrow-linewidth fiber laser and laser diode in unbalanced interferometers," *Chin. Opt. Lett.*, vol. 11, no. 2, 2013, Art. no. 021401.

[21] H. D. Griffiths, "New ideas in FM radar," *Electron. Commun. Eng. J.*, vol. 2, no. 5, pp. 185–194, 1990.

[22] P. Oberson, B. Huttner, O. Guinnard, L. Guinnard, G. Ribordy, and N. Gisin, "Optical frequency domain reflectometry with a narrow linewidth fiber laser," *IEEE Photon. Tech. Lett.*, vol. 12, no. 7, pp. 867–869, Jul. 2000.

[23] M. Harris, G. Constant, and C. Ward, "Continuous-wave bistatic laser doppler wind sensor," *Appl. Opt.*, vol. 40, no. 9, pp. 1501–1506, 2001.

[24] M. Lou, J. Liu, C. Tang, X. Wang, and B. Kan, "0.5 mm spatial resolution distributed fiber temperature and strain sensor with position-deviation compensation based on OFDR," *Opt. Exp.*, vol. 27, no. 24, pp. 35823–35829, 2019.